Journal of Structural Geology, Vol. 8, No. 2, pp. 169 to 180, 1986
Printed in Great Britain

0191-8141/86 $03.00 + 0.00

Microfracturing and regional stress field: a study of the preferred orientations of fluid-inclusion planes in a granite from the Massif Central, France

MARC LESPINASSE

Centre de Recherche sur la Géologie de l'Uranium, 3 Rue du Bois de la Champelle, 54500 Vandoeuvre les Nancy, France

and

ARNAUD PÊCHER

Ecole des Mines, Laboratoire de Géologie Structurale, Parc de Saurupt, 54042 Nancy Cedex, France
and Centre de Recherches Pètrographiques et Géochimiques, B.P. 20, 54501 Vandoeuvre les Nancy, France

(*Received* 16 *January* 1985; *accepted in revised form* 19 *July* 1985)

Abstract—A study of the deformation of a granitic massif indicates a relationship between palaeostress fields and the geometry of microfractures as defined by fluid-inclusion trails, that is, healed microfractures. A statistical study of the distribution of the trails leads to the following conclusions: trails exhibit several distinct preferred orientations on the scale of a grain, which may be observed in many samples; the orientations of the trails are similar to those of micro- and mesoscale fractures in the granite; and the dominant trail direction is parallel to the main direction of regional shortening. Thus, fluid-inclusion trails are mode I cracks which can be used as excellent markers of palaeostress fields.

Résumé—L'étude de la déformation rupturelle d'un massif granitique a permis de mettre en évidence l'existence de relations entre les paléodirections de contraintes et la géométrie d'un marqueur particulier de la microfissuration: les trainées d'inclusions fluides. Une étude statistique de la répartition des trainées d'inclusions fluides montre que: à l'échelle du grain minéral, les trainées ont des orientations préferentielles nettes et régulières d'un échantillon à l'autre; leur réseau est analogue à celui des micro et mésofractures du granite; leur orientation préferentielle principale est parallèle à la direction de raccourcissement majeure régionale. Les trainées d'inclusions fluides sont donc des fractures en mode I qui peuvent être utilisées comme marqueur des paléodirections de contrainte.

INTRODUCTION

WITHIN the last few years, much work has been done on microcracks in rocks. Nevertheless a better understanding of microcrack creation, propagation mechanisms and spatial distribution is necessary, as microcracks affect many physical properties of rocks, such as their strength, seismic wave velocity, and permeability. On the other hand, it can be assumed, as stated by Krantz (1983, pp. 461–462), that ". . . the principles of fracture mechanics will apply to isolated, individual microcrack growth". Thus, microcracks should be capable of yielding valuable information about the local state of stress in rocks. Experimental tests (e.g. Brace & Bombolakis 1963, Friedman & Logan 1970, Peng & Johnson 1972, Tapponnier & Brace 1976, Krantz 1979a,b, 1983) indicate that most cracks appear to be extensional fractures propagated roughly parallel to the local maximum stress axis.

Compared to the rather large quantity of experimental data, only a few papers discuss the relationships between the preferred orientations of cracks and the regional framework of deformational events affecting the surrounding area. There may be only a very weak correlation between each, since grain-scale stress fields are very heterogeneous, depending on the mechanical and thermal anisotropy of the minerals, on grain-boundary geometry, and on older discontinuities in the rock. Nevertheless, some examples can be used to emphasize the regularity on a regional scale of the sets of various joints and fractures.

In a major study within metamorphic rocks near Washington D.C., Tuttle (1949) systematically investigated the orientations of planes of fluid inclusions throughout an area of more than 750 km^2. It appears that these planes, although not clearly related to any particular macroscopic structure, have a remarkably regular, non-random, orientation throughout the metamorphic rocks.

In the same way, Wise (1964) analysed the preferred orientation of microjoints and planes of fluid inclusions in granites of the Precambrian basement of the Montana and Wyoming Rocky Mountains. Here also, these planes appear to form a few constant sets, very regularly orientated across the area, more or less parallel to the common joint directions, but simpler.

Recently, Engelder & Geiser (1980) and Engelder (1982a) described the joint pattern of the Appalachian Plateau, New York. Again, it is astonishingly regular over hundreds of kilometres, and not dependent on other tectonic structures. The youngest set is parallel to the maximum horizontal compression of the present day continental-scale stress field of North America.

Thus these studies point to the use of small-scale

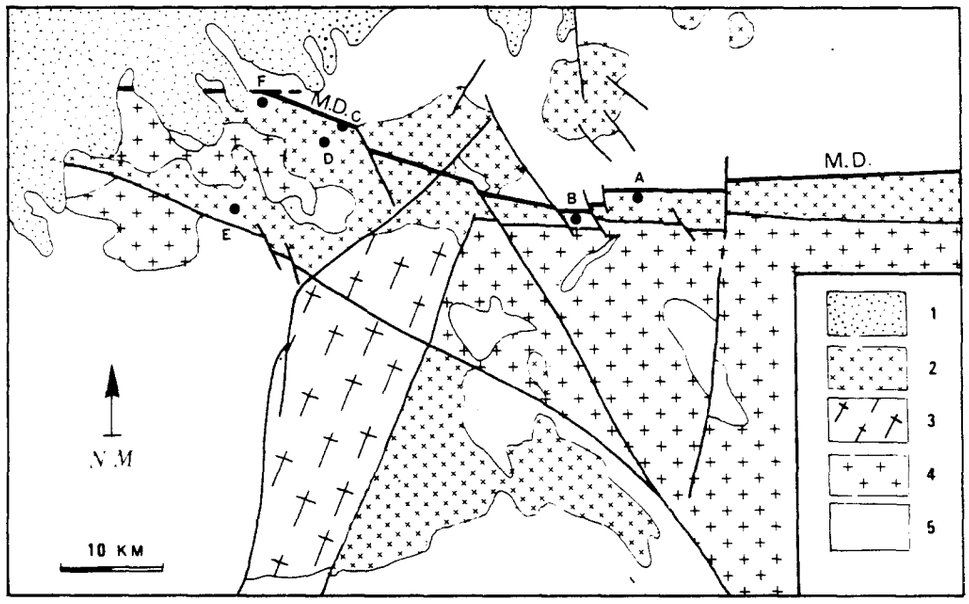

Fig. 1. Sketch map of the western part of the La Marche dislocation. M.D., Marche dislocation; dots, sites of microtectonic measurements (station D corresponds to the Le Bernardan quarry); 1, sedimentary (Jurassic) cover; 2, leucogranites (the northern one, along the Marche dislocation, is the Marche granite, and the southern one is the Saint Sylvestre granite); 3, Brâme foliated leucogranite; 4, Guéret biotite granite; 5, Palaeozoic gneisses and phyllites.

fractures as independent tectonic markers: they appear to be mainly mode I (extensional) cracks formed in response to regional tectonic stress fields. They should yield information on the arrangement of stress trajectories at the time of their formation (see Hancock 1985).

In the present study, dealing with a Hercynian granite in the northwestern part of the Massif Central, France, we have examined the preferred orientations of microfractures versus the successive average regional palaeostress states, as they can be independently determined from the analysis of striated fault planes.

THE GEOLOGICAL FRAMEWORK

Our work derives from a detailed study of the Le Bernardan uranium deposit (Lespinasse 1984) in the La Marche granite. It is a Hercynian two-mica granite, the petrography and geochemistry of which is detailed in Kurtbas *et al.* (1969), Ranchin (1971) and La Roche *et al.* (1980), but the age of which is only poorly known [Rb/Sr dates on the neighbouring biotite–granite of Guéret and two-mica granite of Crevant led respectively to a late Devonian age and to a Namurian age (Berthier *et al.* 1979, Petitpierre & Duthou 1980)]. As in many intragranitic Hercynian uranium deposits, the ore is trapped in hectometric episyenitic columns, which result from potassic alteration and quartz dissolution of the granite by hydrothermal brines, traces of which can be found today in the numerous fluid inclusions which are seen in the granite itself or in quartz veins cutting across it (Michel 1982, 1983, Leroy 1983, 1984).

The La Marche granite is separated from the northern Palaeozoic metamorphic series by a major ductile fault, the so-called 'Marche dislocation' (Fig. 1). It is a thick mylonitic zone, either dipping steeply south, or vertical, which generally trends N90°E, but trends N110°E north of the Le Bernardan quarry. Penetrative deformation textures (appearance of *C-S* almonds, Berthé *et al.* 1979) decrease progressively from the main mylonitic zone to the undeformed granite. In the Le Bernardan quarry, about 1.5 km south of the dislocation, the granite displays only slight traces of deformation: a rough N120°E foliation, emphasized by preferred orientation in phyllites and elongate quartz aggregates (the elongation is due to intracrystalline plastic deformation and some pressure solution).

The episyenitization took place after the plastic deformation, during late Hercynian brittle deformation, when hydrothermal circulation was favoured by the high density of fractures of all scales. For example, the Le Bernardan main episyenitic column is clearly related to a fault breccia orientated N20°E (fault D, Fig. 2). Later still, a stage of fracturing, visible in the granite and gneisses as well as in their Mesozoic cover to the north, occurred after the Jurassic.

THE PALAEOSTRESS FIELD

Several recently developed methods make use of brittle deformation features (joints, veins, striated fault surfaces) to determine the orientations of the palaeostress tensors (see e.g. Angelier 1983, Hancock 1985). Based on a station by station analysis of mesoscopic (i.e. outcrop- and quarry-scale) or macroscopic (map-scale) fractures, these methods average out the sample-scale or grain-scale stress variations. They give an 'average stress state' at each station, from which it is possible to obtain the regional stress pattern by interpolation.

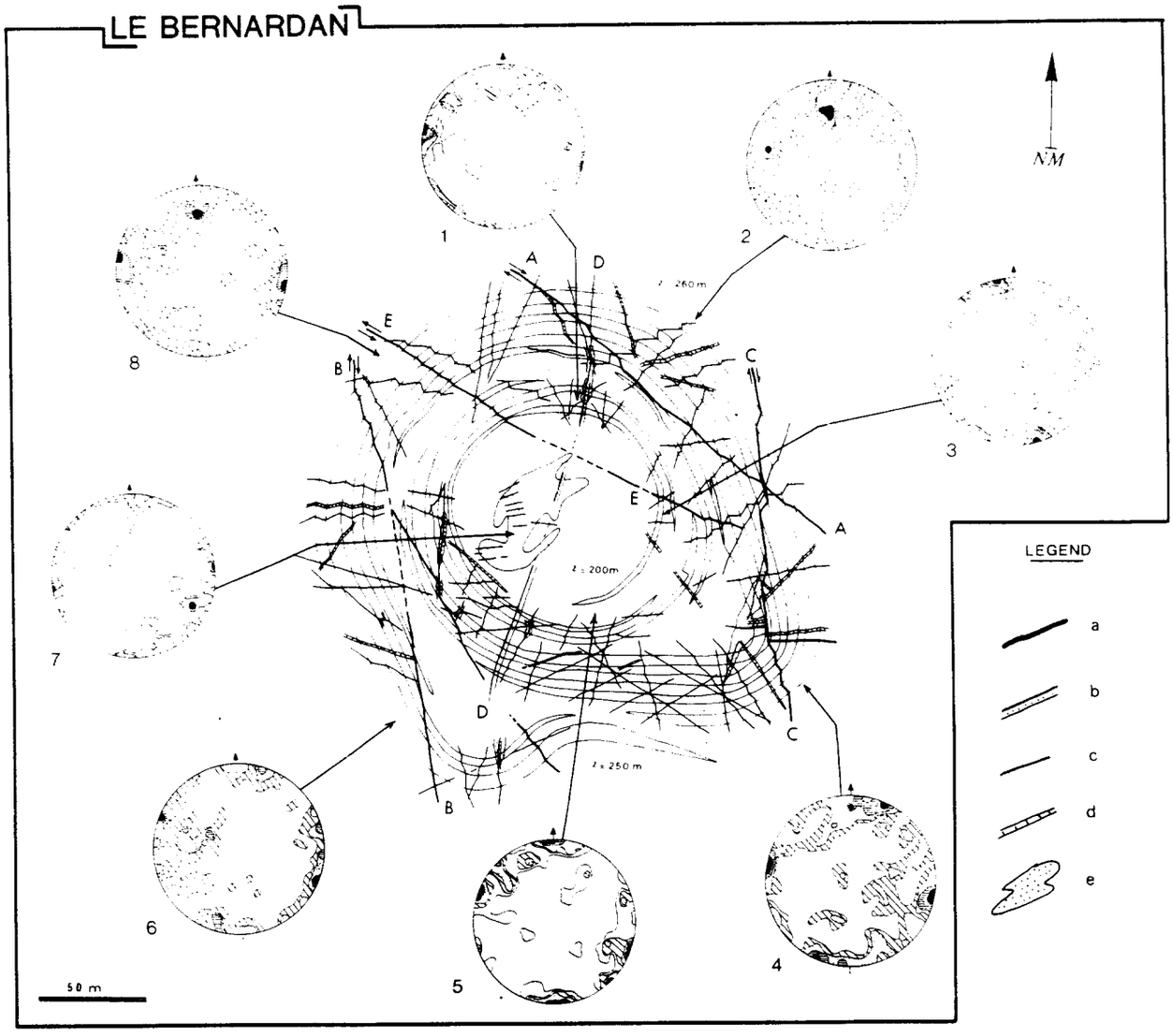

Fig. 2. Sketch map of fractures in the Le Bernardan quarry. a, main faults; b, main N20°E breccia; c, other faults and main joints; d, quartz veins, aplites and pegmatites; e, episyenites. Equal-area plots are for poles to fracture planes; lower hemisphere. 1: 103 measurements (8, 6, 3, 2, 1% density contours). 2: 130 measurements (5, 3, 2, 1% density contours). 3: 123 measurements (7, 5, 3, 2, 1% density contours). 4: 127 measurements (6, 4, 2, 1% density contours). 5: 117 measurements (7, 4, 3, 2, 1% density contours). 6: 150 measurements (6, 4, 3, 1.5% density contours). 7: 114 measurements (6, 4, 2, 1% density contours). 8: 152 measurements (5, 3, 2, 1% density contours).

To determine the palaeostress trajectories in the La Marche granite, we used the computer-aided method proposed by Etchecopar *et al.* (1981), based on Bott's (1959) theory. For a set of striated fractures initiated or reactivated in more than one tectonic phase, the method allows the separation of the main superimposed stress states. 520 fault planes and their striae were measured at six stations (labeled A–F, Figs. 3 and 4), spaced out along 30 km of the La Marche dislocation. Station D is the Le Bernardan quarry.

The six stations give very homogeneous results (an *a posteriori* justification of the mechanical approximations of the method?): the measured striae being related to the superposition at least of three main stress fields, each characterized by an intermediate principal stress, σ_2, which remained close to vertical, and by maximum principal stresses, σ_1, orientated respectively N20°E, N80°E and N150°E.

The more accurately defined direction is the N20°E one (Fig. 3), inferred from 30% of the striations in stations A and B, 15% of the striations in station C, 40% of the striations in station D and 20% of the striations in station E. In the field, the structures are conjugate dextral (N150°E to N180°E) and sinistral (N50°E to N90°E) faults, and N20°E extensional faults. Only at station F was this direction not obtained by the automatic treatment. This does not imply that N20°E compression was ineffective there, but rather it is an effect of the particular location of the station, close to the La Marche dislocation, in a granite strongly foliated along N90°E: the main effect of the N20°E compression was reactivation of the plane of anisotropy (sinistral shear indicated

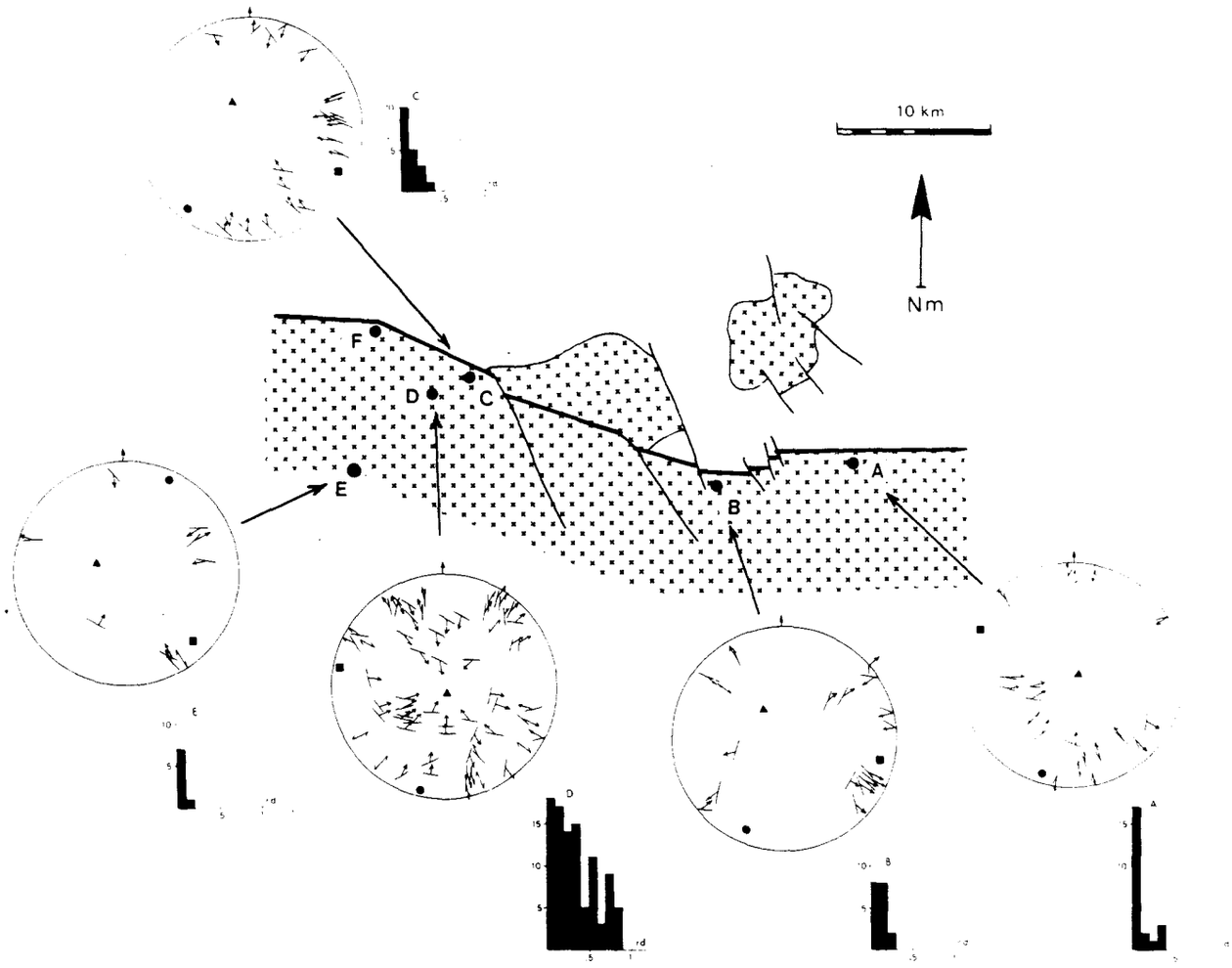

Fig. 3. Palaeostress state in the central and western Marche zone. N20°E compression. Stereographic projection (lower hemisphere) of the corresponding striae. Circles, triangles and squares correspond to σ_1, σ_2 and σ_3 stress axes. The histograms are the residuals between observed and computed striae (see Etchecopar *et al.* 1981); the horizontal axis is scaled in radians. The percentages of measurements for which the deviation is less than 20° (0.34 rd) are 80, 95, 95, 85 and 95% in stations A, B, C, D and E, respectively. $R = (\sigma_2 - \sigma_3)/(\sigma_1 - \sigma_3)$ (see Bott 1959) is equal to 0.74, 0.18, 0.15, 0.33 and 0.38 in A–E.

by slickenside striae). Thus, the data for this station display only a single family of striae compatible with the N20°E direction of compression (the striae on the N90°E foliation in the granite), which is insufficient for stress tensor determination.

The N80°E compression (Fig. 4) is well defined in the five stations A, B, C, D and F. It is marked by dextral movement on N0°E to N50°E faults and sinistral movement on N90°E to N120°E faults.

Finally, a N150°E compression also appears in each of the six stations, but it is rather ill defined because of insufficient striae (no more than 10 per station). Nevertheless, it could be a true regional palaeostress direction: a similar NNW–SSE compression has been inferred from the southern Saint Sylvestre granite (de Fraipont 1982).

The mechanical assumptions used to differentiate the stress tensors do not yield information about their relative order, which can only be established on the basis of criteria such as fault intersections and the superposition of striae. It appears that the N20°E compression occurred first. It was responsible for the late ductile deformation of the granite around 310 Ma (Lespinasse & Pêcher 1984), and later for the emplacement in the Saint Sylvestre granite of N20°E lamprophyre dykes, dated at 295 Ma (Leroy & Sonet 1976). Thus this direction was probably the main regional compression direction from the Viséan to the Stephanian.

It was followed by a N150°E compression. In the Saint Sylvestre granite, it is reflected by dextral N120°E faults, which displace the lamprophyre dykes, by sinistral reactivation of older N–S faults, and by N150°E faults penecontemporaneous with ore deposition (de Fraipont 1982, Lespinasse & Mollier pers. comm.), dated at 275 Ma (Leroy & Holliger 1984). Thus the age of the N150°E compression is probably Stephanian–Autunian.

The N80°E direction is the youngest of the three compression directions. It is defined by faults observed both in the Hercynian basement and in its Mesozoic cover; it is at least partly post-Jurassic, and could be a response to the distant late Alpine mountain building episode (Lerouge *et al.* 1983, Lerouge 1984).

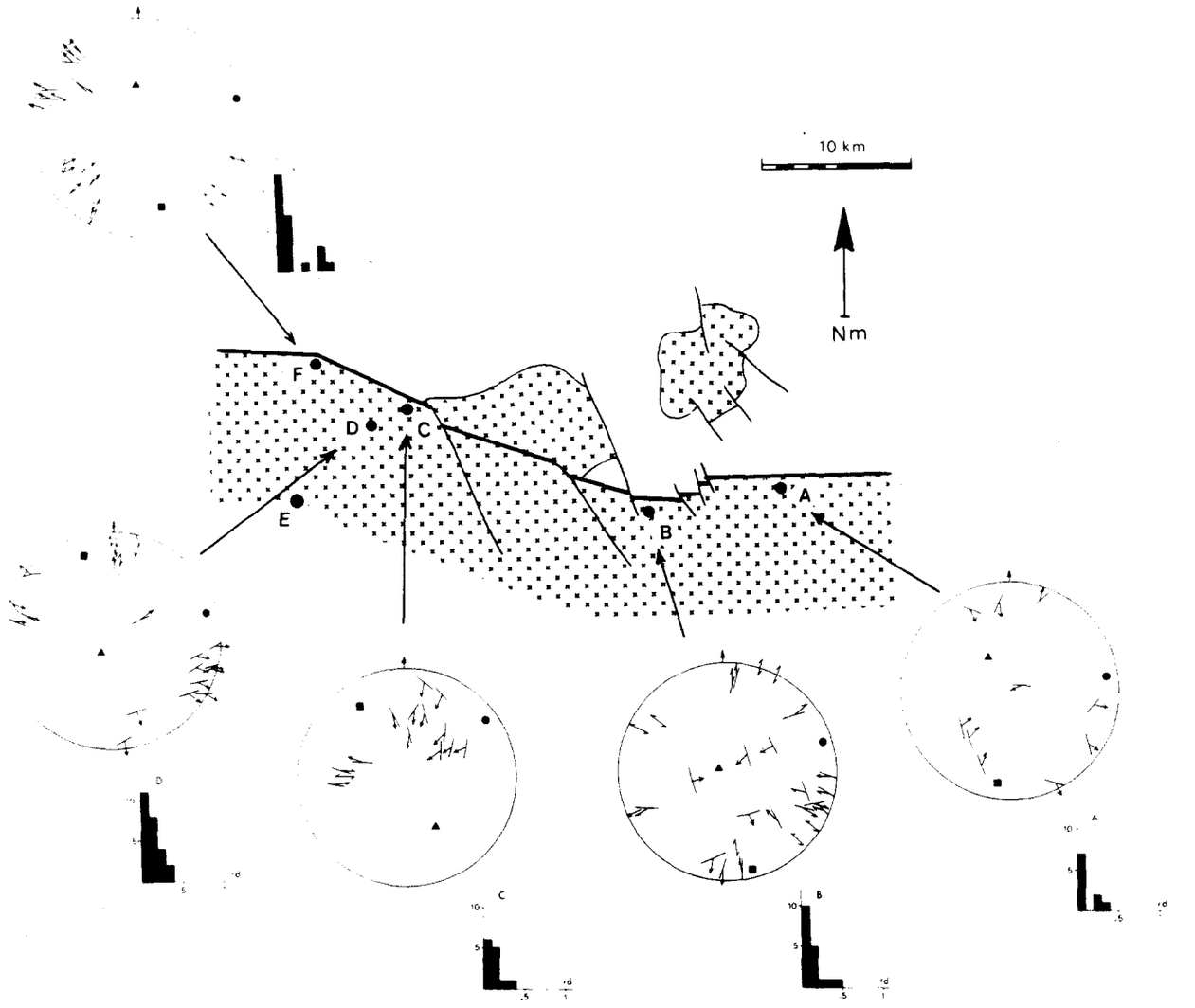

Fig. 4. Palaeostress state in the central and western Marche zone. N80°E compression. Same legend as in Fig. 3. The percentages of measurements for which the deviation is less than 20° are 95, 90, 95, 95 and 75% in stations A, B, C, D and F, respectively. R is equal to 0.21, 0.20, 0.76, 0.36 and 0.78, in A–F.

From the above inference, it is possible to postulate successive patterns of maximum principal stress trajectories (Fig. 5).

MICROFRACTURING

In the Le Bernardan quarry, there is a set of complex metric to pluridecametric faults (Fig. 2), which have been used to determine the average regional stress states defined above. The brittle deformation is also marked by a set of pervasive microfractures of two types, unhealed and healed microcracks.

The unhealed microcracks are intercrystalline cracks (following the terminology of Simmons & Richter 1976) cutting across grain boundaries. They are often large enough to be seen under the microscope at low magnification. A few of them obviously display slight displacements of their two walls, indicated, for example, by displacement of plagioclase twins. There is still controversy over the origin of grain-scale shear cracks and whether some observed shear movements are only due to the reactivation of former mode I (extensional) cracks (see Scheidegger 1982, Engelder 1982b, Hancock 1985). To avoid any ambiguity, only cracks considered as pure extensional cracks, that is, not displaying any evidence of lateral movement, were counted in the statistics presented here.

The healed microcracks, very abundant but only clearly observed in the quartz crystals, are extensional microfractures nearly completely sealed by dendritic growth of quartz from their limbs. Studies by Lemmlein & Kliya (1960), Shelton & Orville (1980), Pêcher (1981), Pêcher & Boullier (1984) and Smith & Evans (1984) indicate that it can be a very fast and effective process. In thin section, or better in the 200 μm thick polished sections used for microthermometric measurements, the healed microcracks appear as thin planar trails of numerous minute (usually less than 10 μm) fluid inclusions, aligned independently of the crystallographic orienta-

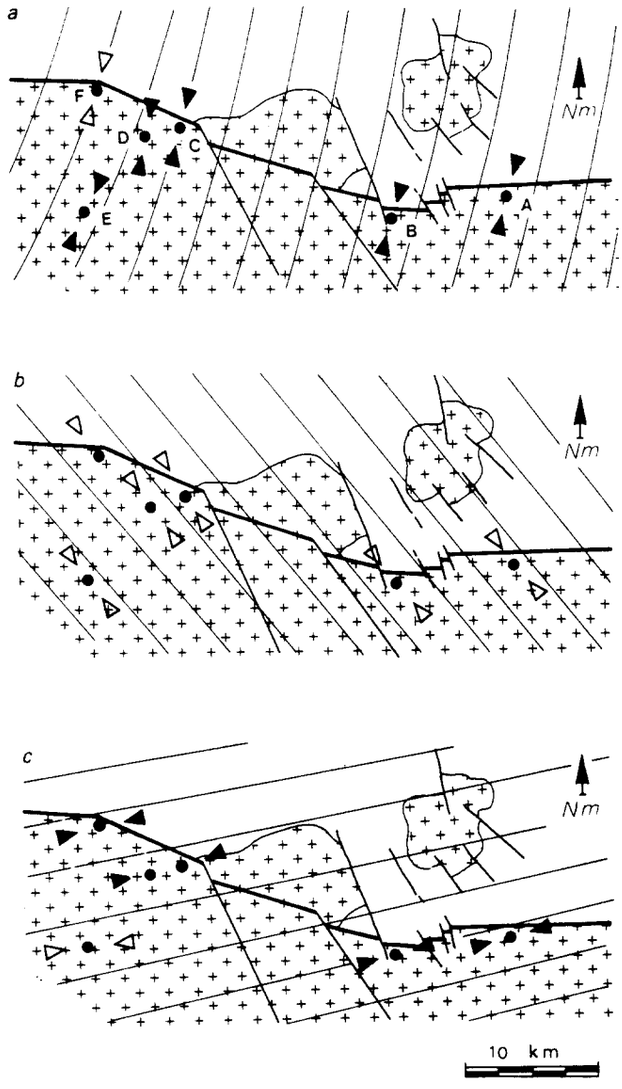

Fig. 5. Successive stress trajectories as determined by striated fault plane analysis. Arrows show the direction of the maximum principal stress, σ_1, at each of the six sampling sites. Solid arrows correspond to well-defined results, open ones to ill-defined results. Lines indicate stress trajectories. (a) N20°E compression (Viséan–Stephanian). (b) N150°E compression (Stephanian–Autunian). (c) N80°E compression (post-Jurassic).

tions of host crystals (as would be trails of primary inclusions), and cross cutting the grain boundaries inherited from ductile deformation. Their maximum length reaches a few mm (Fig. 6).

In this study, the fluid inclusion trails were used as markers of brittle deformation, on the assumption that such sealed cracks do not affect mechanical continuity through the crystal. This is shown, for example, by the evidence for fracturing and healing in granite studied using cathodoluminescence by Sprunt & Nur (1979), or by the repeated parallel, but distinct, fractures in crystals of 'crack–seal' type described by Ramsay (1980). Thus, in the case of superposition of differently orientated stress states, it is anticipated that the set of trails related to one stress state will be essentially unaffected by the geometry of previously formed trails.

Moreover, the composition and density of the fluid trapped in a crack can be estimated simply by microthermometric study of the fluid inclusions, and thus give an idea of the fluid present in the rock at the time of crack sealing. Such studies show (Pêcher *et al.* 1975) that the content of the inclusions was homogeneous along a single trail, but can vary significantly between two differently orientated trails. Thus the included fluids could be either or both traces of local pore fluid (if so, why do we observe different fluids in different trails?), or residues of fluid that has percolated over long distances. Different stages of failure will possibly be distinguished by different types of fluids.

Microfracturing has been studied in 19 samples scattered throughout the 200 m width of the Le Bernardan quarry. Only samples of unaltered granite free of hand-scale fractures were investigated. Most of the microcracks are steep to nearly vertical as can be seen from Fig. 7 (equivalent cyclographic projection of the fluid inclusion trails measured in nine of the samples using a Fedoroff universal stage). Thus, we obtained a good representation of them by taking account only of their traces in horizontal thin-sections. The measurements are presented in rose diagrams, in which the cracks are given in 10° classes. In these diagrams, to gain a more realistic picture of the actual state of microcracks than that given by the stereograms (in which various cracks have the same weight whatever their length), fracture densities were used, that is, the cumulate length of the cracks of similar direction in a given section area (1 cm^2).

Microcracks vs fluid-inclusion trails

To test the preliminary assumption that fluid inclusion trails are equivalent to other microcracks, and to test the homogeneity of fracturing on a specimen scale, measurements of both microcracks and fluid inclusion trails (number of discontinuities of different orientation) were made in four sections of a sample of unaltered granite collected in the wall of a N20°E episyenitic lens (sample ML 82-72).

Figure 8 shows the rather homogeneous fracture pattern of both cracks and fluid inclusion trails. Nevertheless, there is an increase in the number of N20°E fractures from section 4 to section 1; more numerous N20°E fractures occurring closer to the episyenite. Also seen is the very strong similarity of equivalent crack and trail diagrams; it can be seen, for example, that the major N20°E direction is nearly absent in sample ML 82-72c, both in the microcracks and fluid inclusion trails. Thus, the unhealed and healed cracks are equivalent markers, although the reason why some of the cracks are unhealed is unknown. Possibly they were cracks unconnected with the general network of other microfractures, and stayed 'dry' at the time of fluid percolation.

Fluid inclusion trails across the quarry

On the scale of the quarry, plotting the values of the orientations of the fluid inclusion trails on equal-area

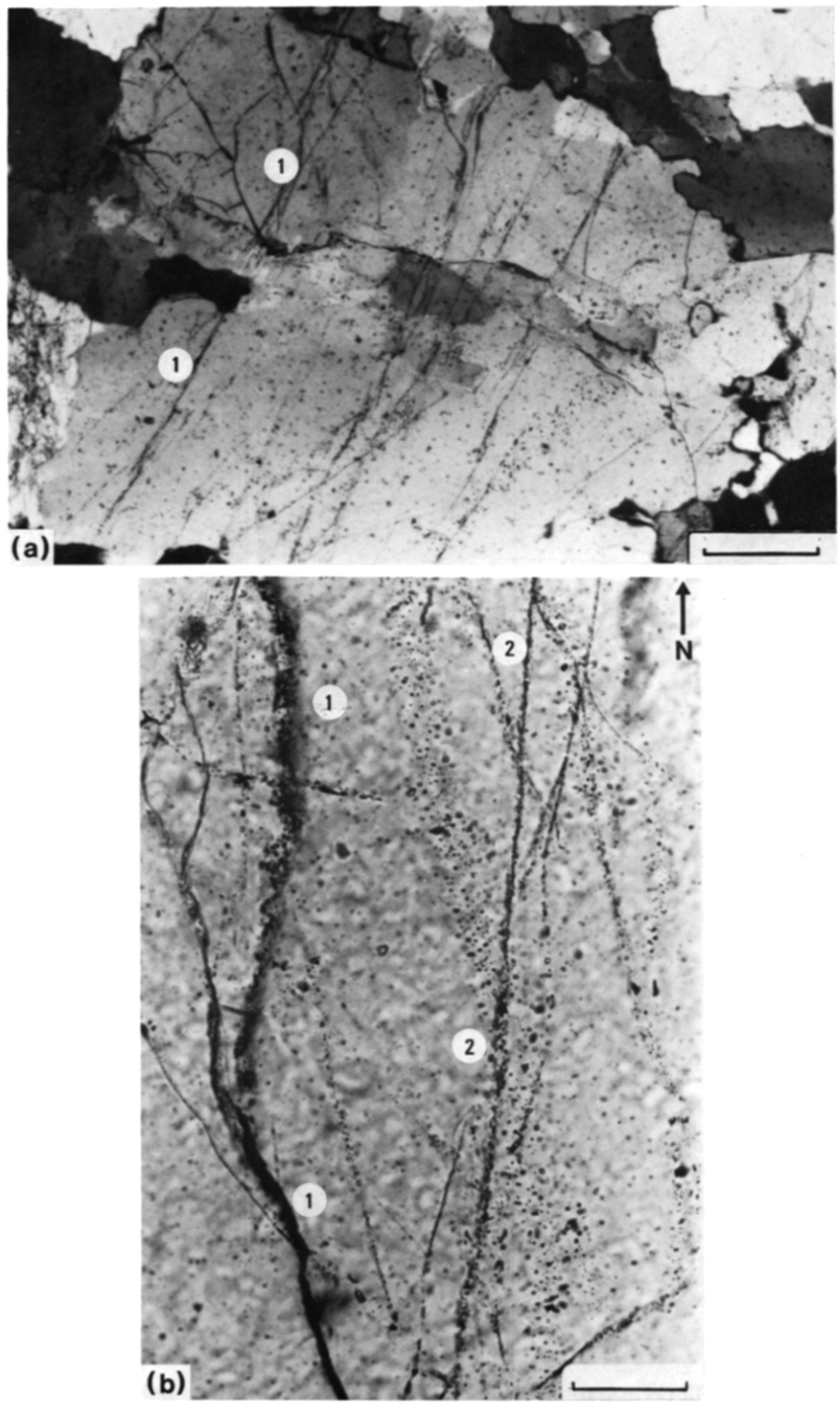

Fig. 6. Photomicrographs of fluid inclusion trails. (a) Relation between polycrystalline quartz and the alignment of fluid inclusions. Scale-bar: 2 mm. Note the regularity of the trail networks (1) and that the trails cut across grain boundaries and are rectilinear. (b) Detail of fluid inclusion trail. 1, microcrack progressively sealed with appearance of fluid inclusions; 2, fluid inclusion trail. Scale bar—0.5 mm.

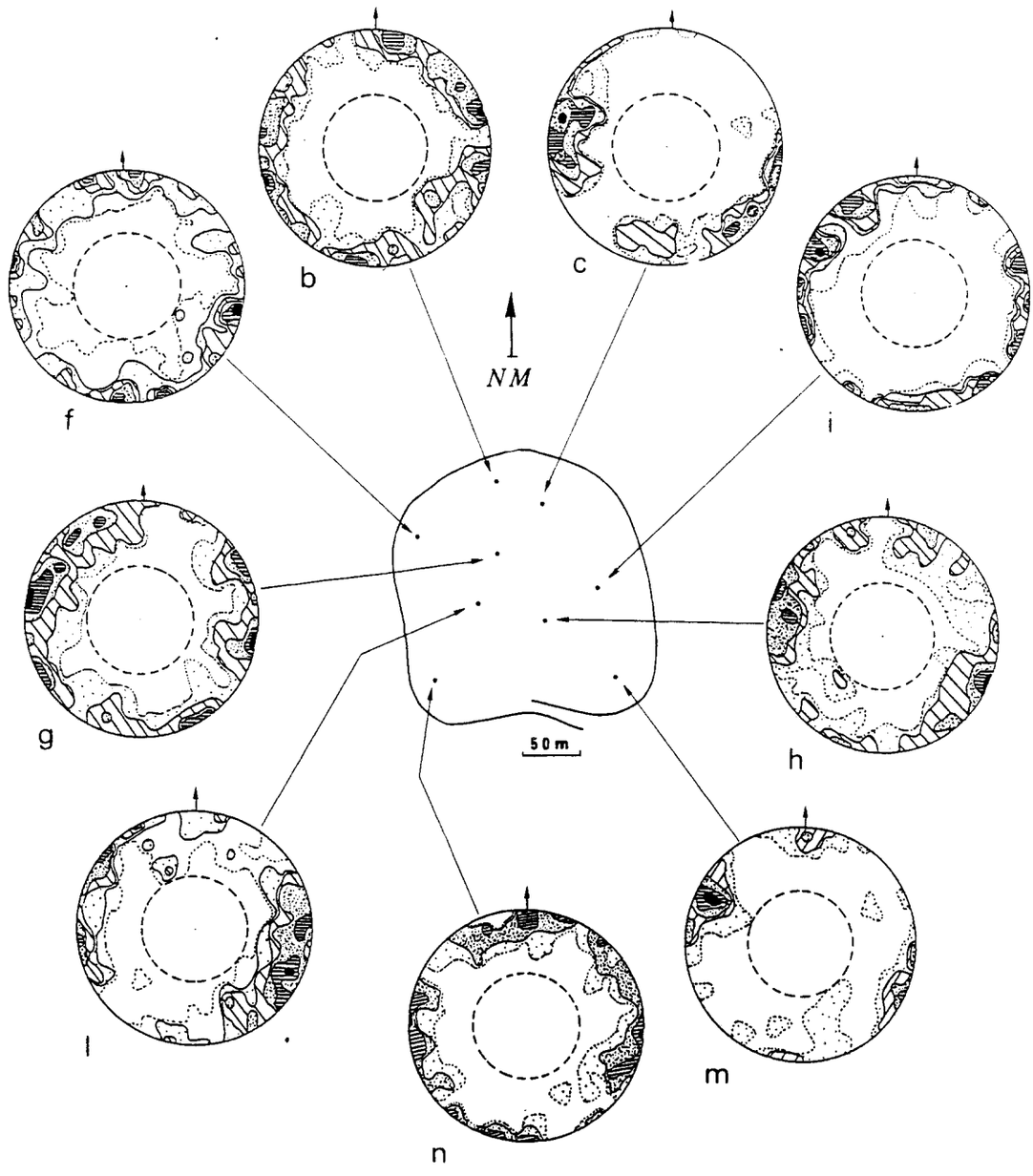

Fig. 7. Orientation of fluid inclusion planes, Le Bernardan quarry. Measurements were obtained with the Fedoroff universal stage and have been plotted on an equal-area counting net, lower-hemisphere projection. For each sample, only one section, cut in a horizontal plane, was used. As a consequence of the geometrical limits of the U-stage such sections do not allow measurement of planes dipping at less than 45° (inner dashed circle). b, sample ML 82 205 (contours at 1, 3, 5 and 7%); c, ML 82 128a (contours at 1, 2, 3, 5 and 8%); f, ML 82 290 (contours at 1, 3, 5, 7 and 10%); g, ML 82 72b (contours at 1, 2, 3, 5 and 8%); h, ML 82 126 (contours at 1, 2, 3, 5 and 8%); i, ML 82 287 (contours at 1, 2, 3, 5 and 7%); l, ML 82 284 (1, 3, 5 and 9%); m, ML 82 91b (contours at 1, 4, 6, 8 and 10%).

counting nets shows the similar orientations of the fluid inclusion trails and mesofractures (cf. Figs. 2 and 7). Rose diagrams (Fig. 9) show more clearly the homogeneity of the microfracture orientations throughout the quarry. A dominant and ubiquitous N20°E direction stands out, together with much less dense, but regular, sets following the N70–80°E, N115°E and N140–160°E directions.

The regularity of the microfracturing is only disturbed in the vicinity of the large A and B faults. As can be seen (Fig. 9), dense N130°E–N160°E microfractures occur near the right-lateral strike-slip fault, A, orientated N120°E; these microfractures are along a compression direction compatible with the sense of movement of the fault. In the same way, a N45°E microfracturing direction appears in samples k and f, close to the N170°E dextral fault, B. In so far as fluid inclusion trails are equivalent to mode-I cracks (that is they should lie close to the position of the local maximum stress), these orientations suggest a local deviation of σ_1 in the vicinity

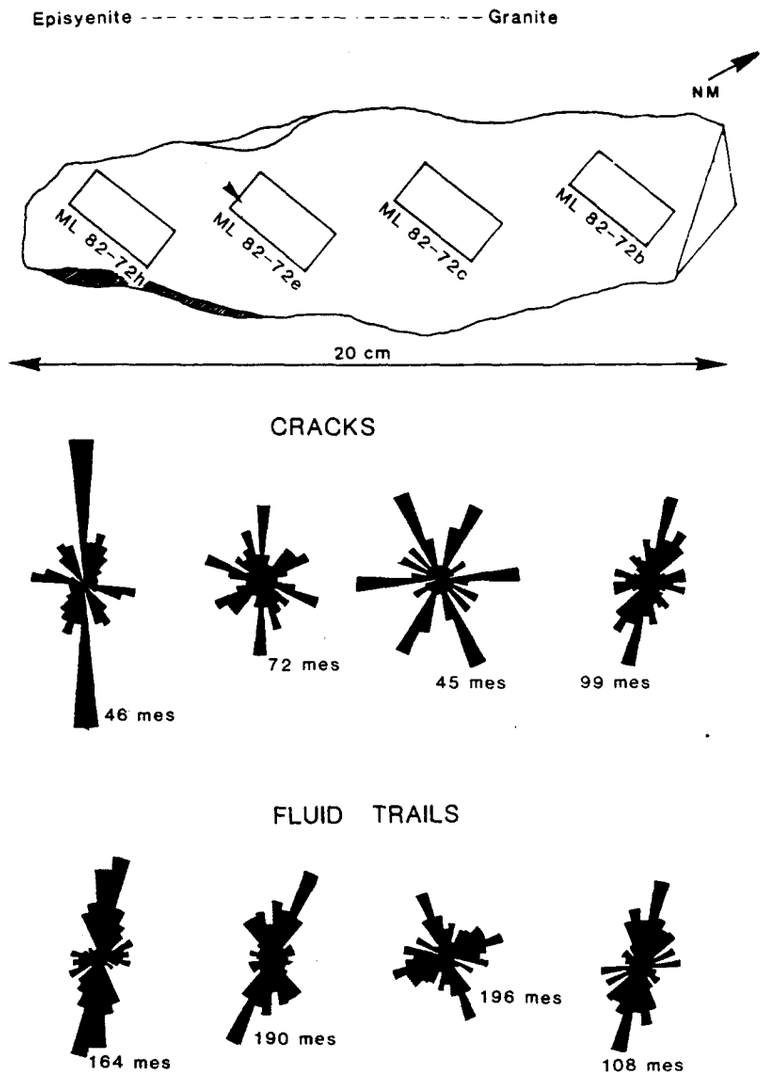

Fig. 8. Comparative rose diagrams of crack and fluid inclusion trail directions. Le Bernardan quarry, sample ML 82 72. Transition between granite and episyenite. Frequence rose diagrams.

of the compressive large faults (2nd-order extensional fracturing accompanying a first-order discontinuity).

Relative timing of various families of trails

Extensional cracks such as fluid inclusion trails display no relative displacement of their walls; thus classical failure chronology criteria, based on intersection displacements, are inappropriate. Because of the lack of geometrical criteria, data on the physico-chemical characteristics of the fluids trapped in the inclusions were employed to erect a chronology. This information is easily obtained by microthermometry, that is measuring under the microscope the melting temperature, *Tm*, which yields the salinity of the fluid, and the homogenization temperature, *Th*, which gives the density of the fluid. Previous studies of fluid associated with episyenitization in the La Marche granite (Leroy 1983, 1984) and in a similar setting [data by Leroy (1978) from the Saint Sylvestre granite] have indicated significant changes in the chemistry and temperature of the hydrothermal fluids during the evolution of the hydrothermal system: for example both temperature and salinity decrease with time.

A microthermometric study of the fluid inclusions in the Le Bernardan granite, taking into account for each inclusion not only its *Th* and *Tm* but also the orientation of the trail in which it is located (Pêcher *et al.* in press), shows that trails of different orientations are characterized by sightly different fluids. In the N20°E trails, salinities of the brine and homogenization temperatures are scattered over a fairly large range of values, but only in these trails can fluids with the highest salinities and the lowest densities be found. The fluid inclusions of the N70°E to N100°E and N140°E to N160°E trails are everywhere filled with very low salinity fluids, whereas their *Th* values are usually lower than the *Th* values measured in the N20°E trails. It is inferred from this data that the N20°E set of trails, in which fluids characteristic of early fluids of a normal episyenitic hydrothermal type

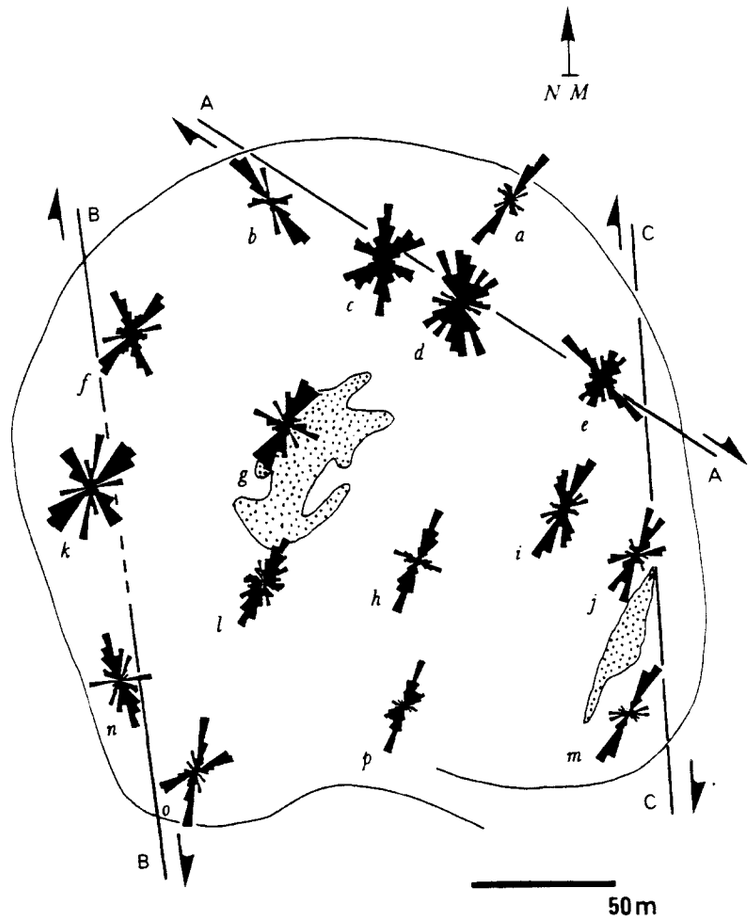

Fig. 9. Preferred orientations of fluid inclusion trails, Le Bernardan quarry. The rose diagrams correspond to the linear density of trails, that is, the total length of trails per unit area (cm^{-1}) in a given direction (10° classes). The three main fractures and the main episyenitic lens (stippled area) are indicated.

are trapped, were the first to be formed, whereas the N80°E and N140°E cracks, in which fluids are characteristic of the late hydrothermal stage, were induced and sealed at a later stage.

CONCLUSIONS

The above description concerns only microcracks in samples collected in the Le Bernardan quarry, that is in a very small part of the La Marche granite (less than 0.05 km^2). Measurements in a few more samples from sites scattered along the whole northern boundary of the La Marche granite, as well as in the Saint Sylvestre granite, further to the south, show that the preferred orientations found on the scale of the quarry are valid on a much wider regional scale (Lespinasse & Mollier, pers. comm.). Below we list our principal conclusions.

(1) Planes of fluid inclusions (fluid inclusion trails), which are believed to have originated as extensional microcracks which subsequently became healed by solution and deposition of silica, have orientations similar to other extensional cracks observed in the granite.

(2) Fluid inclusion trails are aligned along several well-defined directions, remarkably uniformly orientated over large (hectometric, or maybe even kilometric) areas. Thus preferred orientations of trails must be dependent on the average regional stress field and only slightly affected by local heterogeneities.

(3) Successive regional stress trajectories (Fig. 5) compare well with the observed preferred orientations of trails. This correlation cannot be accidental: the early N20°E maximum compressive stress and the N20°E fluid inclusion trails (which seem also to be the oldest from the fluid data) must be related, as well as the N130–150°E and N70–90°E trails with the later N150°E and N80°E maximum compressive stresses.

(4) Fluid inclusion trails are mode I (extensional) cracks which formed parallel to the average direction of σ_1 and perpendicular to the average direction of σ_3 in the bulk rock. Planes of fluid inclusions, typical features in quartz of crystalline rocks, should provide, in the absence of (or in addition to) mesostructural markers, a practical way of constructing extension direction trajectories. Nevertheless, additional work is needed in various tectonic settings to investigate how much the trails deviate from the σ_1 direction, depending on the stress tensor and rock strain characteristics.

(5) The previous assumptions about the preferred orientations of fluid inclusion trails must also be valid for

other types of extensional microcracks (but our data are too few to prove this). Nevertheless, fluid inclusion trails appear to be very useful tools. (a) They do not disrupt the mechanical continuity of mineral grains and thus they may be capable of reflecting slight angular rotations in the direction of the elongation axis. (b) In the context of fluid behaviour during deformation, fluid inclusion trails appear to be fossilized pathways of hydrothermal solution migration. Thus one can use the physico-chemical differences in the included fluids to separate different sets of trails; or, on the other hand, it should be possible to use trails to relate the different stages of fluid percolation to a regional succession of deformational events.

Acknowledgements—This work is based on data collected when one of us (M.L.) was studying the La Marche uranium ore deposit for the Compagnie Minière Dong Trieu. We wish to thank A. Etchécopar, of Montpellier University, who provided us with the computing facilities for the stress tensor determinations, and P. Nehlig, of Strasbourg University, who made some of the microthermometric measurements during a stay at Nancy in the CREGU. T. Engelder, P. L. Hancock and an anonymous reviewer provided many helpful suggestions that improved the manuscript.

REFERENCES

Angelier, J. 1983. Analyses qualitatives et quantitatives des populations de jeux de failles. *Bull. Soc. géol. Fr.* **5**, 661–672.

Berthé, D., Choukroune, P. & Jégouzo, P. 1979. Orthogneiss, mylonite and non coaxial deformation of granites: the example of the South Armorican shear zone. *J. Struct. Geol.* **1**, 31–42.

Berthier, F., Duthou, J. L. & Roques, M. 1979. Datation géochronologique Rb/Sr sur roches totales du granite de Guéret (Massif Central). Age fini-dévonien de mise en place de l'un de ses faciès types. *Bull. Bur. Rech. Géol. min. Fr.* **1/2**, 59–72.

Bott, M. H. P. 1959. The mechanics of oblique slip faulting. *Geol. Mag.* **96**, 107–109.

Brace, W. F. & Bombolakis, E. G. 1963. A note on brittle crack growth in compression. *J. geophys. Res.* **68**, 3709–3713.

Engelder, T. 1982a. Is there a genetic relationship between selected regional joints and contemporary stress within the lithosphere of North America? *Tectonics* **1**, 161–177.

Engelder, T. 1982b. Reply to Scheidegger's comment. *Tectonics* **1**, 5, 465–470.

Engelder, T. & Geiser, P. 1980. On the use of regional joint sets as trajectories of paleostress fields during the development of the Appalachian Plateau, New York. *J. geophys. Res.* **85**, 6319–6341.

Etchécopar, A., Vasseur, G. & Daignières, M. 1981. An inverse problem in microtectonics for determination of stress tensors from fault striation analysis. *J. Struct. Geol.* **3**, 51–65.

de Fraipont, P. 1982. Approche multiscalaire de la fracturation du massif granitique de Saint Sylvestre. Télédétection et analyse tectonique appliquée aux gisements d'uranium de la division minière de la Crouzille, Limousin, Massif Central français. 3rd cycle thesis, Strasbourg.

Friedman, M. & Logan, J. M. 1970. Microscopic feather fractures. *Bull. geol. Soc. Am.* **81**, 3417–3420.

Hancock, P. L. 1985. Brittle microtectonics: principles and practice. *J. Struct. Geol.* **7**, 437–457.

Krantz, R. L. 1979a. Crack growth and development during creep of Barre granite. *Int. J. Rock Mech. Min. Sci.* **16**, 23–35.

Krantz, R. L. 1979b. Crack–crack and crack–pore interactions in stressed granite. *Int. J. Rock Mech. Min. Sci.* **16**, 37–47.

Krantz, R. L. 1983. Microcracks in rocks: a review. *Tectonophysics* **100**, 449–480.

Kurtbas, K., Marquaire, C. & Ranchin, G. 1969. Différenciations pétrographiques et géochimiques dans le massif granitique de Guéret et les massifs annexes de la Marche orientale. *C. r. hebd. Séanc. Acad. Sci., Paris* **268**, 2396–2398.

La Roche, H. de, Stussi, J. M. & Chauris, L. 1980. Les granites à 2 micas hercyniens français. Cartographie et corrélation géochimique avec banque de données. Implications pétrologiques et métallogéniques. Excursion 150, 26th *Int. Geol. Congr.*

Lemmlein, G. C. & Kliya, M. O. 1960. Distinctive features of the healing of a crack in a crystal under conditions of declining temperature. *Int. Geol. Rev.* **2**, 125–128.

Lerouge, G. 1984. Contribution à l'étude de la fracturation du Nord Ouest du Massif Central et du Sud du bassin de Paris. 3rd cycle thesis, Orléans.

Lerouge, G., Quénardel, J. M. & Rolin, P. 1983. La zone de cisaillement de La Marche-Combrailles, son importance dans la tectonique carbonifère du Nord Ouest du Massif Central français. *International Geological Correlation Program*, project 27, Rabat conference.

Leroy, J. 1978. Métallogénèse des gisements d'uranium de la division de La Crouzille (COGEMA, Nord Limousin, France). *Mém. Sci. Terre, Nancy* **36**, 1–278.

Leroy, J. 1983. Le gisement uranifère du Bernardan (Marche, France): exemple d'épisyénitisation d'un granite à deux micas. *C. r. hebd. Séanc. Acad. Sci., Paris* **296**, 75–78.

Leroy, J. 1984. Episyénitisation dans le gisement d'uranium du Bernardan (Marche): comparaison avec des gisements similaires du nord-ouest du Massif Central français. *Miner. Deposita* **19**, 26–35.

Leroy, J. & Holliger, P. 1984. Mineralogical, chemical and isotopic (U-Pb method) studies of Hercynian uraniferous mineralizations (Margnac and Fanay mines, Limousin, France). *Chem. Geol.* **45**, 121–134.

Leroy, J. & Sonet, J. 1976. Contribution à l'étude géochronologique des filons lamprophyres recoupant le granite à deux micas de Saint Sylvestre (Limousin, Massif Central français). *C. r. hebd. Séanc. Acad. Sci., Paris* **283**, 1477–1480.

Lespinasse, M. 1984. Contexte structural des gisements d'uranium de la Marche occidentale. Fracturation, circulations fluides, propagation de l'épisyénitisation. *Géol. Géoch. Uranium, Mém. Nancy* **8**, 1–200.

Lespinasse, M. & Pêcher, A. 1984. Déformation ductile et rupturelle au voisinage de la faille de la Marche: données sur les orientations de raccourcissement tardi-hercyniennes dans le Nord Ouest du Massif Central français. *C. r. hebd. Séanc. Acad. Sci., Paris* **298**, 17–20.

Michel, J. J. 1982. Caractérisations pétrographiques et géochimiques des épisyénitisations uranifères du Bernardan (Haute Vienne, France). *Bull. Soc. géol. Fr.* **7**, 24, 234–248.

Michel, J. J. 1983. Episyénites et concentrations uranifères associées dans le massif de Saint Sulpice les Feuilles. Thesis, Nancy.

Pêcher, A. 1981. Experimental decrepitation and reequilibration of fluid inclusions in synthetic quartz. *Tectonophysics* **78**, 567–584.

Pêcher, A. & Boullier, A. M. 1984. Evolution à pression et température élevées d'inclusions fluides dans un quartz synthétique. *Bull. Minéral.* **107**, 139–153.

Pêchet, A., Lespinasse, M. & Leroy, J. 1985. Relation between fluid inclusion trails and regional stress field: a tool for fluid chronology. The example of an intragranitic uranium ore deposit, North West Massif Central, France. *Lithos* **18**, 229–237.

Peng, S. & Johnson, A. M. 1972. Crack growth and faulting in cylindrical specimens of Chelmsford granite. *Int. J. Rock Mech. Min. Sci.* **9**, 37–86.

Petitpierre, E. & Duthou, J. L. 1980. Age westphalien par la méthode Rb/Sr du leucogranite de Crevant, plateau d'Aigurande (Massif Central français). *C. r. hebd. Séanc. Acad. Sci., Paris* **291**, 163–166.

Ramsay, J. G. 1980. The crack-seal mechanism of rock deformation. *Nature, Lond.* **284**, 137–139.

Ranchin, G. 1971. La géochimie de l'uranium et la différenciation granitique dans la province uranifère du Nord Limousin. *Mém. Sci. Terre Nancy* **19**, 1–394.

Scheidegger, A. E. 1982. Comment on "Is there a genetic relationship between selected regional joints and contemporary stress within the lithosphere of North America" by T. Engelder. *Tectonics* **1**, 463–464.

Shelton, K. L. & Orville, P. M. 1980. Formation of synthetic fluid inclusions in natural quartz. *Am. Min.* **65**, 1233–1236.

Simmons, G. & Richter, D. 1976. Microcracks in rocks. In: *The Physics and Chemistry of Minerals and Rocks* (edited by Strens, R. G. J.). Interscience, New York, 105–137.

Smith, D. L. & Evans, B. 1984. Diffusional crack healing in quartz. *J. geophys. Res.* **89**, 4125–4135.

Sprunt, E. S. & Nur, A. 1979. Microcracking and healing in granites: new evidence from cathodoluminescence. *Science, Wash.* **205**, 495–497.

Tapponnier, P. & Brace, W. P. 1976. Stressed induced microcracks in Westerly granite. *Int. J. Rock Mech. Min. Sci.* **13**, 103–112.

Tuttle, O. F. 1949. Structural petrology of planes of liquid inclusions. *J. Geol.* **57**, 331–356.

Wise, D. U. 1964. Microjointing in basement, Middle Rocky Mountains of Montana and Wyoming. *Bull. geol. Soc. Am.* **75**, 287–306.